Estimation and Compensation of TX and RX IQ Imbalance in OFDM-based MIMO Systems

Tim C.W. Schenk, Peter F.M. Smulders and Erik R. Fledderus
Eindhoven University of Technology, TTE department, PO Box 513, 5600 MB Eindhoven, The Netherlands,
Tel. +31 40 247 3436, Fax. +31 40 245 5197, T.C.W.Schenk@tue.nl.

***Abstract*— This paper studies the influence, estimation and digital compensation of IQ imbalance at both transmitter and receiver side of a multiple-input multiple-output (MIMO) OFDM system. Hereto a preamble is designed, which enables simultaneous estimation of the channel and imbalance parameters. New estimation approaches for TX, RX and joint TX and RX IQ imbalance in MIMO OFDM systems are proposed and evaluated. Results from a numerical study show that all three proposed compensation approaches are able to significantly suppress the influence of IQ mismatch.**

***Index Terms*— MIMO systems, orthogonal frequency division multiplexing (OFDM), IQ imbalance, compensation.**

I. INTRODUCTION

The combination of multiple antenna techniques, often referred to as multiple-input multiple-output (MIMO), with orthogonal frequency division multiplexing (OFDM) is a promising solution for next generation wireless local area networks (WLANs). This solution, however, involves multiple radio front-ends, which requires them to be low-cost. The application of *direct conversion* in both transmitter (TX) as receiver (RX) is then a natural choice, because of the fact that it enables monolithic integration of the analogue front-ends.

One of the problems of these homodyne TXs/RXs, however, is that tolerances in the used components for up/down conversion can easily result in a phase and/or amplitude imbalance between the in-phase (I) and quadrature-phase (Q) signals. This imbalance, referred to as IQ imbalance, can be caused for instance by an error in the 90 degrees phase shift in the up/down conversion, but also by imbalances between the other parts of the I and Q branches.

This paper presents data-aided approaches for estimation and compensation of the imbalance parameters. Differently from previous work for single antenna systems, e.g. [1–3], this work regards IQ mismatch at both sides of the fading channel. New algorithms are derived for TX, RX and joint TX and RX IQ imbalance estimation in MIMO OFDM systems. The performance is evaluated using Monte-Carlo simulations of an IEEE 802.11a-based MIMO system.

II. INFLUENCE OF TX AND RX IQ IMBALANCE

Consider a multiple-antenna based OFDM system with N_t TX and N_r RX branches. The system applies N subcarriers of which $2K$ carriers contain data symbols.

When we consider frequency flat IQ imbalance, we can extend the results from [4] to show that for a MIMO OFDM system impaired by TX and RX IQ imbalance the received $N_r \times 1$ signal vector on the kth carrier during the mth symbol, $\mathbf{X}_{m,k}$, is given by

$$\mathbf{X}_{m,k} = \left(\mathbf{K}_1\mathbf{H}_k\mathbf{G}_1 + \mathbf{K}_2\mathbf{H}^*_{-k}\mathbf{G}_2\right)\mathbf{s}_{m,k} + \left(\mathbf{K}_2\mathbf{H}^*_{-k}\mathbf{G}^*_1 + \mathbf{K}_1\mathbf{H}_k\mathbf{G}^*_2\right)\mathbf{s}^*_{m,-k} \ , \quad (1)$$

for $k \in \{-K, \ldots, -1, 1, \ldots, K\}$. Here $\mathbf{H}_k$ denotes the $N_r \times N_t$ quasi-static channel transfer matrix for the kth subcarrier and * denotes complex conjugation. The $N_t \times 1$ transmit symbol vector is denoted by $\mathbf{s}_{m,k}$. It can be concluded from (1) that the received signal on the kth carrier is a combination of the MIMO signal vectors transmitted on carrier k and on its mirror carrier $-k$. In (1) the TX IQ imbalance is contained in the $N_t \times N_t$ matrices $\mathbf{G}_1$ and $\mathbf{G}_2$ and the RX IQ imbalance in the $N_r \times N_r$ matrices $\mathbf{K}_1$ and $\mathbf{K}_2$, which are defined as

$$\mathbf{G}_1 = (\mathbf{I} + \boldsymbol{g}_\mathrm{T} e^{j\boldsymbol{\phi}_\mathrm{T}})/2 \ , \qquad \mathbf{G}_2 = \mathbf{I} - \mathbf{G}^*_1 \ , \quad (2)$$

$$\mathbf{K}_1 = (\mathbf{I} + \boldsymbol{g}_\mathrm{R} e^{-j\boldsymbol{\phi}_\mathrm{R}})/2 \ , \qquad \mathbf{K}_2 = \mathbf{I} - \mathbf{K}^*_1 \ , \quad (3)$$

where $\mathbf{I}$ denotes the identity matrix. The imbalance matrices are defined as

$$\boldsymbol{\phi}_\mathrm{X} = \mathrm{diag}\{\phi_{\mathrm{X},1}, \phi_{\mathrm{X},2}, \ldots, \phi_{\mathrm{X},N_x}\} \ , \quad (4)$$

$$\boldsymbol{g}_\mathrm{X} = \mathrm{diag}\{g_{\mathrm{X},1}, g_{\mathrm{X},2}, \ldots, g_{\mathrm{X},N_x}\} \ , \quad (5)$$

where $\mathrm{X} \in \{\mathrm{T}, \mathrm{R}\}$ and $N_x \in \{N_t, N_r\}$. Here $g_{\mathrm{X},n}$ and $\phi_{\mathrm{X},n}$ are the amplitude and phase imbalance for the nth branch, respectively. When there are no imbalances, these parameters equal 1 and 0, respectively.

III. ESTIMATION / COMPENSATION APPROACH

A. Preamble design

To enable estimation of the MIMO channel transfer and the IQ imbalance matrices in (2) and (3), we propose a data-aided approach. The estimation is enabled by a preamble, i.e., a piece of known data preceding the data transmission. The proposed preamble is schematically depicted in Fig. 1 for a MIMO system with two transmit branches.

TX1	$\mathbf{d}_1$	$\mathbf{d}_2$	$\mathbf{d}_1$	$\mathbf{d}_2$	DATA 1
TX2	$\mathbf{d}_1$	$\mathbf{d}_2$	$-\mathbf{d}_1$	$-\mathbf{d}_2$	DATA 2

Fig. 1. Transmission format for a system with 2 TX branches.

This preamble is a MIMO extension of what was proposed for a single-input single-output (SISO) system in [3]. It applies Hadamard sequences to create orthogonality between subcarriers pairs k and $-k$ and between the different TX branches. The orthogonality in the spatial domain is apparent from transmission structure in Fig. 1 and can, since it applies Hadamard sequences, easily be extended for more TX branches. The orthogonality between the carriers is achieved by the design of $\mathbf{d}_1$ and $\mathbf{d}_2$. Hereto, the symbols on the kth carrier of $\mathbf{d}_1$ and $\mathbf{d}_2$ are given by

$$d_{1,k} \in \{-1,1\} \quad \text{for all } k \quad , \tag{6}$$

$$d_{2,k} = \begin{cases} d_{1,k} & \text{for } k \in \{1,2,\ldots,K\} \\ -d_{1,k} & \text{for } k \in \{-K,-K+1,\ldots,-1\} \end{cases} , \tag{7}$$

respectively.

When this preamble is applied for conventional MIMO channel estimation, two joint wireless channel/IQ imbalance transfer matrices are found for every carrier, i.e., $\mathbf{C}_k^+$ and $\mathbf{C}_k^-$. These are obtained when the signs of the training symbols on carrier k and $-k$ are equal and different, respectively. The transfer matrices are given by

$$\mathbf{C}_k^+ = \mathbf{K}_1\mathbf{H}_k(\mathbf{G}_1+\mathbf{G}_2^*) + \mathbf{K}_2\mathbf{H}_{-k}^*(\mathbf{G}_1^*+\mathbf{G}_2) \quad , \tag{8}$$

$$\mathbf{C}_k^- = \mathbf{K}_1\mathbf{H}_k(\mathbf{G}_1-\mathbf{G}_2^*) + \mathbf{K}_2\mathbf{H}_{-k}^*(\mathbf{G}_2-\mathbf{G}_1^*) \quad . \tag{9}$$

From (8) and (9) we can, subsequently, find the channel and frequency flat IQ imbalance parameters using the algorithms presented in Sections III-B to III-D.

B. TX IQ mismatch

When we first regard a system only impaired by TX IQ imbalance, the expressions for the estimated transfer matrices in (8) and (9) reduce to

$$\mathbf{C}_k^+ = \mathbf{H}_k \quad , \tag{10}$$

$$\mathbf{C}_k^- = \mathbf{H}_k(\mathbf{G}_1-\mathbf{G}_2^*) = \mathbf{H}_k\mathbf{g}_\mathrm{T}\exp(j\boldsymbol{\phi}_\mathrm{T}) \quad . \tag{11}$$

Now we can estimate the imbalance vectors $\boldsymbol{\phi}_\mathrm{T}$ and $\boldsymbol{g}_\mathrm{T}$ for the kth carrier as

$$\boldsymbol{\phi}_{\mathrm{T},k} = \arctan\left(\Im\{\mathbf{C}_k^{+\dagger}\mathbf{C}_k^-\}\Re\{\mathbf{C}_k^{+\dagger}\mathbf{C}_k^-\}^{-1}\right) \quad , \tag{12}$$

$$\boldsymbol{g}_{\mathrm{T},k} = \sqrt{\Re\{\mathbf{C}_k^{+\dagger}\mathbf{C}_k^-\}^2 + \Im\{\mathbf{C}_k^{+\dagger}\mathbf{C}_k^-\}^2} \quad , \tag{13}$$

where † denotes the pseudo-inverse and where $\Re\{\cdot\}$ and $\Im\{\cdot\}$ give the real and imaginary part of their arguments.

Improved estimates of these imbalance parameters are obtained by averaging over the frequency index k, which exploits the frequency independence of the IQ imbalance. A further improvement is achieved by making use of the fact that the IQ parameters are time-invariant. This can be done by averaging the imbalance parameters with those found in the previous P packets. This averaging over time and frequency yields the improved estimates $\bar{\boldsymbol{g}}_\mathrm{T}$ and $\bar{\boldsymbol{\phi}}_\mathrm{T}$.

Now the imbalance parameters have been estimated, the MIMO channel matrix for the kth carrier can be found by

$$\mathbf{H}_k = \frac{\mathbf{C}_k^+ + \mathbf{C}_k^-(\bar{\boldsymbol{g}}_\mathrm{T}\exp(j\bar{\boldsymbol{\phi}}_\mathrm{T}))^{-1}}{2} \quad . \tag{14}$$

The estimated parameters, i.e., $\bar{\boldsymbol{\phi}}_\mathrm{T}$, $\bar{\boldsymbol{g}}_\mathrm{T}$ and $\mathbf{H}_k$, are used during the data phase to correct the received signals for the IQ imbalance and to detect the transmitted symbols.

C. RX IQ mismatch

When a system which only experiences RX IQ mismatch is considered, (8) and (9) reduce to

$$\mathbf{C}_k^+ = \mathbf{K}_1\mathbf{H}_k + \mathbf{K}_2\mathbf{H}_{-k}^* \quad , \tag{15}$$

$$\mathbf{C}_k^- = \mathbf{K}_1\mathbf{H}_k - \mathbf{K}_2\mathbf{H}_{-k}^* \quad . \tag{16}$$

We subsequently define

$$\mathbf{C}_{k,\mathrm{s}} = (\mathbf{C}_k^+ + \mathbf{C}_k^-)/2 \quad , \tag{17}$$

$$\mathbf{C}_{k,\mathrm{d}} = (\mathbf{C}_k^+ - \mathbf{C}_k^-)/2 \quad , \tag{18}$$

$$\mathbf{Q}_k = \left(\mathbf{C}_{k,\mathrm{s}} - \mathbf{C}_{-k,\mathrm{d}}^*\right)\left(\mathbf{C}_{k,\mathrm{s}} + \mathbf{C}_{-k,\mathrm{d}}^*\right)^\dagger \quad , \tag{19}$$

and since $\mathbf{Q}_k$ can be written as $\boldsymbol{g}_\mathrm{R}\exp(-j\boldsymbol{\phi}_\mathrm{R})$, the imbalance parameters for the kth carrier are found by

$$\boldsymbol{\phi}_{\mathrm{R},k} = -\angle\mathbf{Q}_k = -\arctan\left(\Im\{\mathbf{Q}_k\}\Re\{\mathbf{Q}_k\}^{-1}\right) \tag{20}$$

$$\boldsymbol{g}_{\mathrm{R},k} = |\mathbf{Q}_k| = \sqrt{\Re\{\mathbf{Q}_k\}^2 + \Im\{\mathbf{Q}_k\}^2}. \tag{21}$$

Again, the estimates can be improved by averaging over the estimates obtained at the different subcarriers and P previous packets, yielding $\bar{\boldsymbol{\phi}}_\mathrm{R}$, $\bar{\boldsymbol{g}}_\mathrm{R}$ and $\bar{\mathbf{Q}} = \bar{\boldsymbol{g}}_\mathrm{R}\exp(-j\bar{\boldsymbol{\phi}}_\mathrm{R})$.

The estimate of the MIMO channel matrix for the kth subcarrier is then found to be

$$\mathbf{H}_k = \frac{(\mathbf{C}_{k,\mathrm{s}} + \mathbf{C}_{-k,\mathrm{d}}^*) + \bar{\mathbf{Q}}^{-1}(\mathbf{C}_{k,\mathrm{s}} - \mathbf{C}_{-k,\mathrm{d}}^*)}{2}, \tag{22}$$

which provides us with the parameters to estimate.

D. TX and RX IQ mismatch

When the MIMO OFDM system experiences both TX and RX IQ imbalance, the estimation problem can not be solved directly. Hereto (8) and (9) are simplified by making the following approximations

$$\mathbf{G}_1 \pm \mathbf{G}_2^* \approx \mathbf{G}_1 \qquad \text{and} \qquad \pm\mathbf{G}_1^* + \mathbf{G}_2 \approx \pm\mathbf{G}_1^* \quad , \tag{23}$$

which are valid for small values of TX IQ imbalance. The expressions for the MIMO transfer matrices in (8) and (9) then reduce to

$$\hat{\mathbf{C}}_k^+ = \mathbf{K}_1\mathbf{H}_k\mathbf{G}_1 + \mathbf{K}_2\mathbf{H}_{-k}^*\mathbf{G}_1^* \quad , \tag{24}$$

$$\hat{\mathbf{C}}_k^- = \mathbf{K}_1\mathbf{H}_k\mathbf{G}_1 - \mathbf{K}_2\mathbf{H}_{-k}^*\mathbf{G}_1^* \quad . \tag{25}$$

Applying these approximate expressions, the RX imbalance parameters can be estimated. Hereto we define

$$\hat{\mathbf{C}}_{k,\mathrm{s}} = (\hat{\mathbf{C}}_k^+ + \hat{\mathbf{C}}_k^-)/2 = \mathbf{K}_1\mathbf{H}_k\mathbf{G}_1 \quad , \tag{26}$$

$$\hat{\mathbf{C}}_{k,\mathrm{d}} = (\hat{\mathbf{C}}_k^+ - \hat{\mathbf{C}}_k^-)/2 = \mathbf{K}_2\mathbf{H}_{-k}^*\mathbf{G}_1^* \quad . \tag{27}$$

Subsequently, we find for the kth subcarrier

$$\begin{aligned}\hat{\mathbf{Q}}_k &= (\hat{\mathbf{C}}_{k,\mathrm{s}} - \hat{\mathbf{C}}_{-k,\mathrm{d}}^*)(\hat{\mathbf{C}}_{k,\mathrm{s}} + \hat{\mathbf{C}}_{-k,\mathrm{d}}^*)^\dagger \\ &= \boldsymbol{g}_\mathrm{R}\exp(-j\boldsymbol{\phi}_\mathrm{R}) \quad .\end{aligned} \tag{28}$$

The RX phase and amplitude imbalance matrices are then easily found from (28) as

$$\boldsymbol{\phi}_{\mathrm{R},k} = -\arctan\left(\Im\{\hat{\mathbf{Q}}_k\}\Re\{\hat{\mathbf{Q}}_k\}^{-1}\right) \quad , \tag{29}$$

$$\boldsymbol{g}_{\mathrm{R},k} = \sqrt{\Re\{\hat{\mathbf{Q}}_k\}^2 + \Im\{\hat{\mathbf{Q}}_k\}^2} \quad . \tag{30}$$

Improved estimates of the imbalance parameters can be obtained by averaging over time and frequency, yielding $\bar{g}_R$, $\bar{\phi}_R$ and $\bar{\mathbf{Q}} = \bar{g}_R \exp(-j\bar{\phi}_R)$.

Following this we can go back to the original expressions in (8) and (9). Using these expressions and the estimated RX IQ imbalance parameters, the MIMO channel matrix for the kth carrier is found to be given by

$$\mathbf{H}_k = (\bar{\mathbf{Q}} + \bar{\mathbf{Q}}^*)^{-1}(\bar{\mathbf{Q}}^*(\mathbf{C}_k^+ + {\mathbf{C}_{-k}^+}^*) + \mathbf{C}_k^+ - {\mathbf{C}_{-k}^+}^*). \quad (31)$$

Finally, to estimate the TX IQ imbalance parameters, we rewrite (9) for carrier k and its mirror $-k$ in matrix notation as

$$\begin{bmatrix} \mathbf{C}_k^- \\ \mathbf{C}_{-k}^- \end{bmatrix} = \underbrace{\begin{bmatrix} \mathbf{K}_1\mathbf{H}_k & \mathbf{K}_2\mathbf{H}_{-k}^* \\ \mathbf{K}_1\mathbf{H}_{-k} & \mathbf{K}_2\mathbf{H}_k^* \end{bmatrix}}_{\mathbf{T}_k} \begin{bmatrix} \mathbf{g}_T e^{j\phi_T} \\ -\mathbf{g}_T e^{-j\phi_T} \end{bmatrix}. \quad (32)$$

It is then easily found that

$$\begin{bmatrix} \mathbf{M}_{1,k} \\ \mathbf{M}_{2,k} \end{bmatrix} = \begin{bmatrix} \mathbf{g}_T e^{j\phi_T} \\ -\mathbf{g}_T e^{-j\phi_T} \end{bmatrix} = \hat{\mathbf{T}}_k^\dagger \begin{bmatrix} \mathbf{C}_k^- \\ \mathbf{C}_{-k}^- \end{bmatrix}, \quad (33)$$

where $\hat{\mathbf{T}}_k$ is constructed from the estimated channel and RX IQ parameters, derived in the previous steps. From (33) the TX IQ imbalance parameters for the kth subcarrier are estimated as

$$\boldsymbol{\phi}_{T,k} = \arctan\left(\Im\{\mathbf{M}_{1,k} - \mathbf{M}_{2,k}^*\}\Re\{\mathbf{M}_{1,k} - \mathbf{M}_{2,k}^*\}^{-1}\right), \quad (34)$$

$$\boldsymbol{g}_{T,k} = \frac{\sqrt{\Re\{\mathbf{M}_{1,k} - \mathbf{M}_{2,k}^*\}^2 + \Im\{\mathbf{M}_{1,k} - \mathbf{M}_{2,k}^*\}^2}}{2}. \quad (35)$$

Again, the improved estimates of the imbalance parameters, i.e., $\bar{\boldsymbol{\phi}}_T$ and $\bar{\boldsymbol{g}}_T$, are obtained by averaging the imbalance estimates over the subcarriers and the previous P packets.

IV. NUMERICAL RESULTS

Monte-Carlo simulations were performed to test the performance of the estimation approaches presented in Sections III-B to III-D. This section presents results from this numerical study, which were carried out for a 2×2 MIMO extension of the IEEE 802.11a standard [5]. The channel is modeled as quasi-static, i.e., the channel is constant over the length of the packet, but generated independently for the different packets. Furthermore, the power-delay-profile is exponential decaying with a rms delay spread of 50 ns. The spatial channels are i.i.d. and the fading is Rayleigh distributed.

Figure 2 depicts results for the mean-squared-error (MSE) in estimation of the TX IQ imbalance parameters by the algorithm proposed in Section III-B. The system experienced TX IQ imbalance with $\boldsymbol{\phi}_T = \text{diag}\{3°, -3°\}$ and $\boldsymbol{g}_T = \text{diag}\{1.1, 0.9\}$ and no RX IQ imbalance. Averaging over P received packets is applied to improve the performance.

It can be concluded from Fig. 2 that the MSE (in degrees^2) in estimation of $\boldsymbol{\phi}_T$ decreases linearly (on log-scale) with SNR. When the number of packets is increased, the MSE decreases even further. As regards the estimation of $\boldsymbol{g}_T$ it can be concluded that for $P = 1$ the MSE decreases linearly with SNR. When averaging of the IQ parameters over P packets is applied, the MSE only improves linearly as function of P

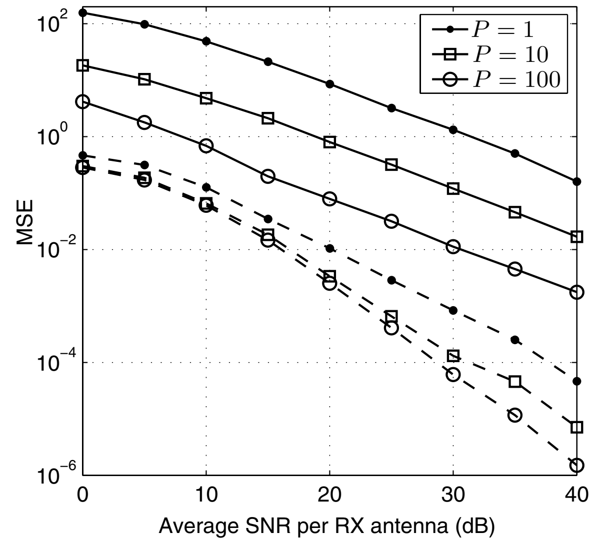

Fig. 2. MSE in estimation of the diagonal elements of $\boldsymbol{\phi}_T$ (solid lines) and $\boldsymbol{g}_T$ (dashed lines) applying TX IQ imbalance estimation (Section III-B).

for high SNR. For low SNR a bias in the estimation seems to limit the performance.

Similar MSE results are depicted in Fig. 3, but now for a system only experiencing RX IQ imbalance and applying the estimation approach of Section III-C. The imbalance parameters were $\boldsymbol{\phi}_R = \text{diag}\{3°, -3°\}$ and $\boldsymbol{g}_R = \text{diag}\{1.1, 0.9\}$.

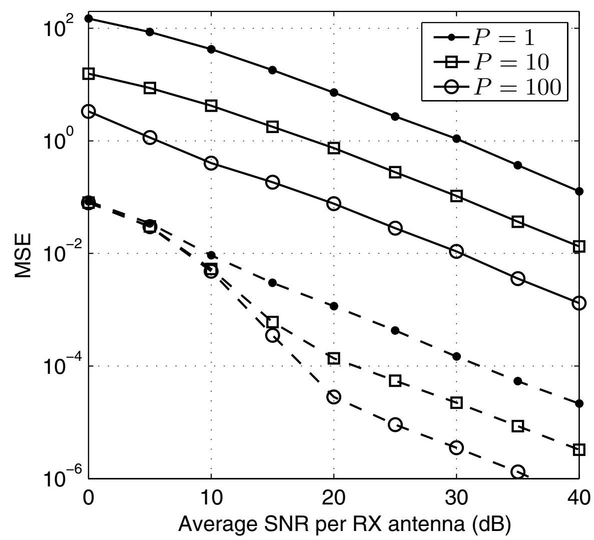

Fig. 3. MSE in estimation of the diagonal elements of $\boldsymbol{\phi}_R$ (solid lines) and $\boldsymbol{g}_R$ (dashed lines) applying RX IQ imbalance estimation (Section III-C).

The MSE results in Fig. 3 are very similar to those in Fig. 2. The bias in estimation of RX amplitude imbalance seems to limit the performance less for than for the case of TX imbalance.

MSE results for a system impaired by both TX and RX IQ imbalance ($\boldsymbol{\phi}_T = \text{diag}\{1°, -1°\}$, $\boldsymbol{\phi}_R = \text{diag}\{3°, -3°\}$, $\boldsymbol{g}_T = \text{diag}\{1.05, 0.95\}$ and $\boldsymbol{g}_R = \text{diag}\{1.1, 0.9\}$) and applying the joint TX and RX imbalance estimation of Section III-D are depicted in Fig. 4. It can be concluded from this figure that the MSE in estimation of all imbalance matrices show flooring at high SNR values due to the approximations made in (23). The MSE is greatly improved by averaging over P = 100 packets, however, the flooring remains.

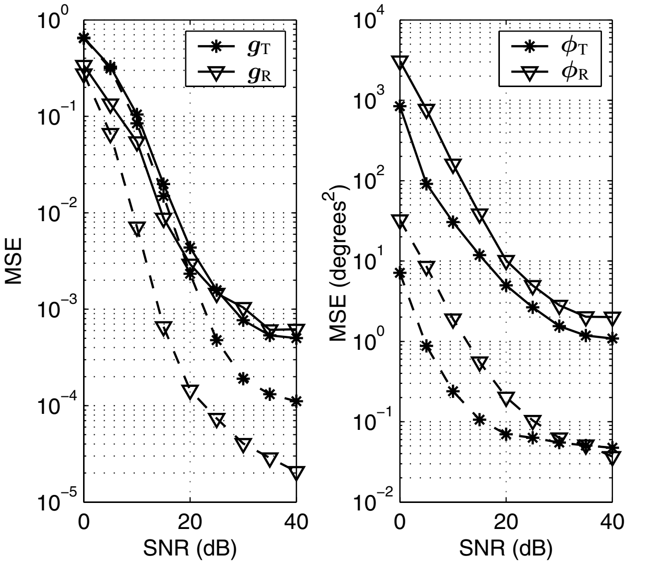

Fig. 4. MSE in estimation of TX and RX IQ imbalance parameters for P=1 (solid lines) and P=100 (dashed lines) applying joint TX and RX IQ imbalance estimation (Section III-D).

Results from bit-error-rate (BER) simulations are presented in Fig. 5 and Fig. 6 for a 2×2 MIMO system applying Zero-Forcing (ZF) estimation with 64-QAM modulation and no coding. The imbalance estimation and compensation approaches of Section III-C and Section III-D are applied. Reference curves are given for a system not applying IQ imbalance compensation, and for a system not impaired by IQ imbalance.

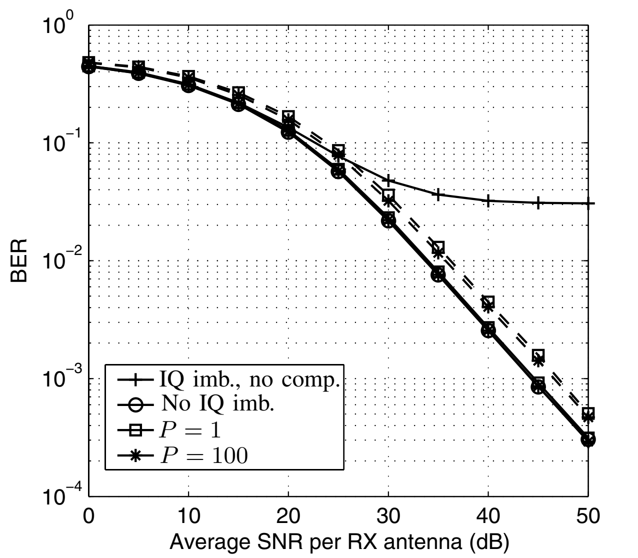

Fig. 5. BER performance of a 2×2 ZF-based system in detection of 64-QAM data for a system experiencing RX IQ imbalance ($\phi_R = \text{diag}\{3°, -3°\}$ and $g_R = \text{diag}\{1.1, 0.9\}$). The estimation approaches of Section III-C (solid lines) and III-D (dashed lines) are applied.

It can be concluded from Fig. 5 that the influence of RX IQ imbalance without compensation is severe and limits the system performance significantly. For the estimation of Section III-C the BER performance resembles that of a system without IQ imbalance. Averaging over more packets does not increase the performance further, since the influence of the noise is dominant over that of the remaining IQ imbalance after compensation. For the joint estimation approach of Section III-D the BER performance is a little improved when the number packets is increased, however, a difference of 1.5 dB compared to the ideal curve remains, due to the higher channel estimation errors for this approach.

For the case of both TX and RX IQ imbalance in Fig. 6 we conclude that also here considerable improvement in BER performance is achieved by the proposed approach. More packets are required, however, to achieve a similar performance to that in Fig. 5. Again a difference of 1.5 dB compared to the ideal case (with no IQ imbalance) remains, even for a high number of packets P. Results for systems applying other MIMO detectors and/or coding are similar, but shifted to another (lower) SNR range.

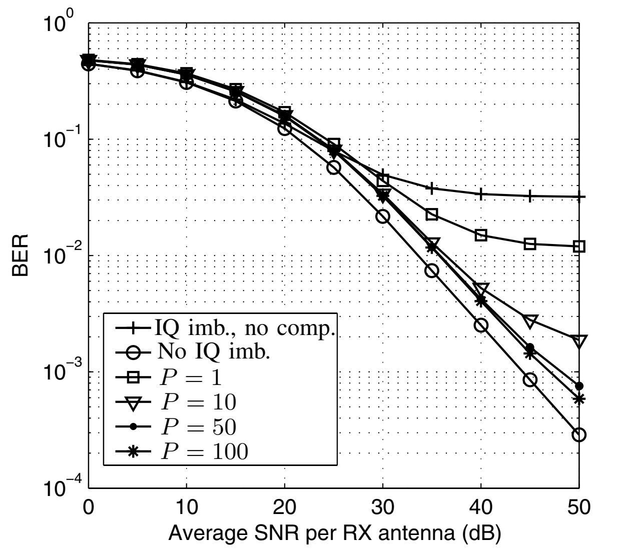

Fig. 6. BER performance of a 2×2 ZF-based system in detection of 64-QAM data for a system experience TX and RX IQ imbalance ($\phi_T = \text{diag}\{1°, -1°\}$, $\phi_R = \text{diag}\{3°, -3°\}$, $g_T = \text{diag}\{1.05, 0.95\}$ and $g_R = \text{diag}\{1.1, 0.9\}$). The estimation approach of Section III-D is applied.

V. Conclusions

The influence of transmitter and receiver-induced IQ mismatch is studied in this paper. Three data-aided estimation and compensation approaches are proposed for the case of transmitter, receiver and transmitter and receiver IQ imbalance. These approaches exploit that the imbalance parameters are time-invariant. A numerical performance study shows the mean-squared-error performance of the different estimation algorithms. Results from bit-error-rate simulations show that the proposed algorithms can significantly reduce the influence of IQ mismatch.

References

[1] J. Tubbax et al., "Compensation of IQ imbalance in OFDM systems," in *Proc. IEEE International Conference on Communications 2003*, vol. 5, May 2003, pp. 3403–3407.

[2] M. Windisch and G. Fettweis., "Standard-independent I/Q imbalance compensation in OFDM direct-conversion receivers," in *Proc. 9th International OFDM Workshop*, Sept. 2004.

[3] L. Brötje, S. Vogeler, K.-D. Kammeyer, R. Rueckriem, and S. Fechtel, "Estimation and correction of transmitter-caused I/Q imbalance in OFDM systems," in *Proc. 7th International OFDM Workshop*, Sept. 2002.

[4] M. Valkama, M. Renfors, and V. Koivunen, "Advanced methods for I/Q imbalance compensation in communication receivers," *IEEE Trans. on Signal Proc.*, vol. 49, 2001.

[5] A. v. Zelst and T. Schenk, "Implementation of a MIMO OFDM-based wireless LAN system," *IEEE Trans. on Sign. Proc.*, vol. 52, no. 2, pp. 483–494, Feb. 2004.